Published in final edited form as:
J Neurosci. 2011 June 29; 31(26): 9563–9573. doi:10.1523/JNEUROSCI.1701-11.2011.

Sapap3 deletion anomalously activates short-term endocannabinoid-mediated synaptic plasticity

Meng Chen[1], **Yehong Wan**[1], **Kristen Ade**[1], **Jonathan Ting**[2], **Guoping Feng**[2,3], and **Nicole Calakos**[1,2,*]

[1] Center for Translational Neuroscience, Dept. of Medicine/Neurology, Duke University Medical Center, Durham, NC 27710

[2] Dept. of Neurobiology, Duke University Medical Center, Durham, NC 27710

[3] McGovern Institute for Brain Research, Department of Brain and Cognitive Sciences, Massachusetts Institute of Technology, Cambridge, MA 02139

Abstract

Retrograde synaptic signaling by endocannabinoids is a widespread mechanism for activity-dependent inhibition of synaptic strength in the brain. Although prevalent, the conditions for eliciting endocannabinoid (eCB)-mediated synaptic depression vary among brain circuits. As yet, relatively little is known about the molecular mechanisms underlying this variation, although the initial signaling events are likely dictated by postsynaptic proteins. SAPAPs are a family of postsynaptic proteins unique to excitatory synapses. Using *Sapap3* knock-out (KO) mice, we find that, in the absence of SAPAP3, striatal medium spiny neuron (MSN) excitatory synapses exhibit eCB-mediated synaptic depression under conditions that do not normally activate this process. The anomalous synaptic plasticity requires type 5 metabotropic glutamate receptors (mGluR5), which are dysregulated in *Sapap3* KO MSNs. Both surface expression and activity of mGluR5 are increased in *Sapap3* KO MSNs, suggesting that enhanced mGluR5 activity may drive the anomalous synaptic plasticity. In direct support of this possibility, we find that, in wildtype (WT) MSNs, pharmacological enhancement of mGluR5 by a positive allosteric modulator is sufficient to reproduce the increased synaptic depression seen in *Sapap3* KO MSNs. The same pharmacologic treatment, however, fails to elicit further depression in KO MSNs. Under conditions that are sufficient to engage eCB-mediated synaptic depression in WT MSNs, *Sapap3* deletion does not alter the magnitude of the response. These results identify a role for SAPAP3 in the regulation of postsynaptic mGluRs and eCB-mediated synaptic plasticity. SAPAPs, through their effect on mGluR activity, may serve as regulatory molecules gating the threshold for inducing eCB-mediated synaptic plasticity.

Keywords

endocannabinoid; basal ganglia; synaptic plasticity; SAPAP3; metabotropic glutamate receptors

INTRODUCTION

The postsynaptic scaffold of proteins is important for synapse formation and dynamic modification of postsynaptic signaling. As such, these proteins can regulate neurotransmitter receptor activity. Scaffold proteins effectively link the major neurotransmitter receptors to

*Correspondence should be addressed to Nicole Calakos, PO Box 2900, Duke University Medical Center, Durham, NC 27710. nicole.calakos@duke.edu.

intracellular signaling cascades and cytoskeletal elements (Sheng and Pak, 1999; Rumbaugh et al., 2003; Kim and Sheng, 2004). SAP90/PSD-95-associated proteins (SAPAPs, also referred to as guanylate kinase-associated proteins or GKAPs) are a family of postsynaptic scaffold proteins that localize to an intermediate layer of the postsynaptic density (PSD) (Kim et al., 1997; Takeuchi et al., 1997; Valtschanoff and Weinberg, 2001) and are unique to excitatory synapses (Welch et al., 2004). By virtue of the protein complexes in which SAPAPs have been identified *in vitro* (Naisbitt et al., 1997; Boeckers et al., 1999; Tu et al., 1999; Hirao et al., 2000; Romorini et al., 2004), SAPAPs might influence the activity of ionotropic and metabotropic glutamate receptors and/or the intracellular signaling cascades with which these receptors interact. However, to date, very little is known about whether SAPAPs influence synaptic activity.

SAPAPs are encoded by a family of four genes that are widely expressed throughout the nervous system (Takeuchi et al., 1997; Kindler et al., 2004; Welch et al., 2004). In prior studies, we have shown that SAPAP3 KO mice have Obsessive Compulsive Disorder (OCD)-like behaviors (excessive self-grooming, facial lesions, anxiety-like behaviors and therapeutic response to fluoxetine) and altered basal striatal neurotransmission (Welch et al., 2007). SAPAP3 is the only SAPAP that is highly expressed in the striatum (Welch et al., 2004; Welch et al., 2007). Viral rescue of SAPAP3 expression in the striatum of SAPAP3 KO mice prevents the behavioral abnormalities and reverses the striatal neurotransmission defects demonstrating that striatal loss of SAPAP3 activity is critical for the expression of the pathological behaviors. These findings indicate that, at striatal synapses, SAPAP3 has little functional redundancy with other SAPAPs. Accordingly, the study of excitatory synaptic function in the striatum of *Sapap3* KO mice provides a unique platform for elucidating the role of SAPAPs in synaptic function.

In this study, we investigate excitatory synaptic transmission of striatal medium spiny neurons (MSNs) in acute brain slices from *Sapap3* KO mice. We find that loss of SAPAP3 results in abnormal endocannabinoid-mediated synaptic plasticity. Striatal excitatory synapses of *Sapap3* KO mice engage eCB-mediated, short-term synaptic depression under conditions that are insufficient to activate this process in wild-type (WT) synapses. This is likely due to an increase in group 1 mGluR activity. Group 1 mGluR activity and mGluR5 surface expression are increased in *Sapap3* KO MSNs. Pharmacological enhancement of mGluR5 activity in WT MSNs mimics the abnormal synaptic depression of KO MSNs. These findings provide the first functional evidence for a role of SAPAP3 in the regulation of postsynaptic mGluRs and eCB-mediated synaptic plasticity.

MATERIALS AND METHODS

Animals

Generation of *Sapap3* KO mice, *Drd1a*-tdTomato transgenic mice, and *Drd2*-EGFP transgenic mice has been previously described (Gong et al., 2003; Welch et al., 2007; Shuen et al., 2008). Experimental mice were the progeny of $Sapap3^{+/-} \times Sapap3^{+/-}$ breedings in which only one of the parents expressed the *Drd1a*-tdTomato or *Drd2*-EGFP transgenes so that no experimental subjects were homozygous for the transgenic fluorescent markers. In experiments testing genotype effects, littermate control animals were used. All experiments were performed and analyzed with the experimenter blind to the identity of the experimental variable being tested (i.e. genotype or drug effect). *CB1R* KO mice were provided by Dr. Rui Costa and generated by Dr. Andreas Zimmer (Zimmer et al., 1999). All animal procedures were done according to protocols approved by the Institutional Animal Care and Use Committee of Duke University.

Brain slice preparation

Coronal brain slices (300 μm) were used for all recording and imaging experiments. In extracellular recording experiments, Sapap3$^{+/+}$ and $^{-/-}$ mice aged 3 – 12 weeks old and Sapap3$^{-/-}$/CB1R$^{-/-}$ and Sapap3$^{-/-}$/CB1R$^{+/+}$ mice aged 24 – 52 weeks old were used. Sapap3$^{+/+}$ and $^{-/-}$ mice co-expressing *Drd1a*-tdTomato and/or *Drd2*-EGFP transgenes were used for whole-cell recording experiments (3 weeks old) and calcium dye imaging experiments (2.5 weeks old). All electrophysiological results are from 3 week-old mice, unless otherwise specified. Young mice were anesthetized with isoflurane prior to decapitation. Older mice (> 8 weeks) were anesthetized with tribromo-ethanol and transcardially perfused with oxygenated, ice-cold ACSF prior to decapitation. The brain was rapidly removed and sliced in oxygenated, ice-cold sucrose artificial cerebral spinal fluid (ACSF) with a Vibratome 1500 (Leica, USA). Sucrose ACSF contained (in mM): 194 sucrose, 30 NaCl, 2.5 KCl, 1.2 NaH_2PO_4, 0.2 $CaCl_2$, 2 $MgCl_2$, 26 $NaHCO_3$, and 10 D-(+)-glucose (Choi and Lovinger, 1997). Slices recovered in standard ACSF saturated with 95% O_2 and 5% CO_2 at room temperature for at least 1 hour before recording. Standard ACSF contained (in mM): 124 NaCl, 2.5 KCl, 1.2 NaH2PO4, 2 CaCl2, 1 MgCl2, 26 NaHCO3, and 10 D-(+)- glucose.

Electrophysiology—Slices were continuously perfused at a constant rate of 2–3 mL/min with standard ACSF saturated with 95% O_2 and 5% CO_2. Recordings were made in the dorsolateral region of striatum and stimulation was given in the corpus callosum. Stimuli were programmed by pClamp software (Axon Instruments, USA) and delivered using an Iso-flex stimulus isolator (A.M.P.I., Israel) and a twisted tungsten wire bipolar electrode (A-M systems, OD: 0.005 inches) (Lovinger and McCool, 1995). MultiClamp 700B amplifier and DigiData 1322A (Axon Instruments) were used for signal acquisition. Signals were sampled at 20 kHz and low-pass filtered at 2 kHz. Picrotoxin (50 μM) was present in all experiments to exclude $GABA_A$ inhibitory synaptic activity. Experiments were performed at 30 – 32°C unless otherwise specified.

For field potential recordings, the recording pipette was filled with 2 M NaCl and pipette resistance was approximately 1–3 MΩ. The basal stimulation intensity was selected by identifying the lowest intensity that elicited the maximal field potential amplitude determined by an input/output survey performed at room temperature. Field potential responses were evoked using paired stimuli (50 ms inter-pulse interval [IPI]). For whole-cell, voltage-clamp recordings, membrane potential was held at −70 mV unless otherwise specified. Recording pipettes had a resistance of 2.5 – 4.5 MΩ when filled with internal pipette solution containing (in mM): 120 Cs-$MeSO_3$, 5 NaCl, 10 TEA-Cl, 10 HEPES, 0.3 EGTA, 4 MgATP, 0.3 Na_3GTP and 5 QX314-Cl. The osmolarity was adjusted to ~290 mOsm/L with sucrose and the pH was adjusted to 7.3 with cesium hydroxide. Cells were visualized with a 40× water immersion objective (LUMPlanFI, 40×/0.80w) under an Olympus BX51WI microscope equipped with infrared differential interference contrast (IR-DIC) optics, reflected fluorescence system, and OLY-150 camera (Olympus). Series resistance (R_s) was monitored continuously by a 5 mV voltage step following each pair of evoked excitatory postsynaptic currents (eEPSC). Average series resistance (R_s), input membrane resistance (R_m), holding current (I_{hold}) and membrane capacitance (C_m) were: R_s (MΩ) – WT, 16.8 ± 2.0, n = 13; KO, 20.3 ± 1.6, n =14; p = 0.2; R_m (MΩ) – WT, 240 ± 20, n = 13; KO, 307 ± 35, n = 14; p = 0.1; I_{hold} (pA) – WT, −27 ± 9, n = 13; KO, −13 ± 7, n = 14; p = 0.2; C_m (pF) – WT, 100 ± 4, n = 13; KO, 87 ± 6, n = 14; p = 0.1. Recordings with Rs > 30 MΩ or a change of >20% were excluded. EPSCs were evoked using paired stimuli (50 ms IPI). The basal stimulation intensity was adjusted to elicit baseline EPSC amplitudes between 200 – 400 pA. Paired-pulse ratios (PPR) were calculated by the ratio of the averaged peak of the second EPSC (or population spike, PS) to the averaged peak of the first

EPSC (or PS) for each 60 second time period. All responses were normalized to the average value during the 7.5 min period of 90 s interval stimulation just prior to stimulation interval change ("baseline"). Summary bar graphs of activity-dependent depression protocol data present the average value during the last 10 minutes of 10 s stimulation normalized to baseline. Dose eliciting sub-maximal effect of (*R*)-(+)-[2,3-Dihydro-5-methyl-3-(4-morpholinylmethyl)pyrrolo[1,2,3-*de*]-1,4-benzoxazin-6-yl]-1-naphthalenylmethanone mesylate (WIN 55212-2) was identified in pilot experiments which tested a range of drug concentrations (0.3 – 6 μM) to determine a concentration of WIN 55212-2 that produced a sub-maximal level of depression. At 6 μM, a maximal degree of depression (eEPSC amplitude relative to baseline – 55 ± 9%, $n = 4$) was observed. Long-term depression (LTD) experiments were performed at 30 s basal stimulation interval. LTD was induced by four 100 Hz trains of 1 s duration paired with depolarization to 0 mV (Choi and Lovinger, 1997; Kreitzer and Malenka, 2005). Inter-train interval was 10 s. Stimulus intensity during high frequency stimulation (HFS) was increased to the minimum intensity that evoked the maximal field response (Kreitzer and Malenka, 2005). Sample traces are the average of 5 consecutive sweeps. In all experiments reporting response amplitude, the values refer to the amplitude of the first response elicited by the pair of 50 ms IPI stimuli.

Calcium imaging in acute brain slices

Acute coronal brain slices (300 μM) were prepared from P17–19 WT and KO littermates expressing both *Drd1a*-tdTomato and *Drd2*-EGFP transgenes. One hour after sectioning, slices were transferred to incubation chambers containing 3 mL standard ACSF equilibrated with 95% O_2 and 5% CO_2 and maintained at 36°C for calcium indicator bulk loading (MacLean and Yuste, 2009). The FURA2-AM dye solution was prepared daily by dissolving 50 μg of FURA2-AM (Invitrogen) in 22 μL DMSO/Pluronic F-127 (0.02%, Invitrogen). Nine μL of filtered dye solution was added to each incubation chamber for bulk loading of the slices. After 30 minutes, the slices were transferred to a holding chamber containing standard ACSF at room temperature for at least 45 minutes prior to imaging. All imaging was completed within 3 hours of the loading procedure. Dye preparation as well as loading, recovery and imaging of the slices were performed in the dark to minimize photo-bleaching of the FURA2-AM.

After recovery from the loading procedure, slices were transferred to the imaging chamber on an upright Ultima microscope (Prairie Technologies). Fields of view 50 ± 20 μm deep in the dorsolateral striatum were selected for imaging, and a femtosecond laser (Chameleon Ultra I, Coherent Technologies) was used to excite the transgenic and calcium indicator fluorophores. The laser wavelength was tuned to 1040 nm for tdTomato and 900 nm for EGFP. FURA2-AM was imaged with a single wavelength (800 nm) which predominately excites FURA-2 in a calcium-free state (Wokosin et al., 2004; Nikolenko et al., 2008). Fluorescence images were acquired using Prairie View image acquisition software (Prairie Technologies). Emitted photons were collected by a 20X 1.0 NA XLUMPlanFL N water immersion objective and an Aplanat/Acrhromatic 1.4 NA oil immersion condenser (Olympus) and redirected to both epi- and trans-fluorescence photomultiplier systems where emitted light was split into two channels by a 575 nm dichroic mirror. EGFP and fura-2AMsignals were imaged a 525/70 nm bandpass filter. TdTomato signal was imaged using a 607/45 nm bandpass filter.

After acquiring EGFP and tdTomato reference images, FURA-2 fluorescence raster-scan images were acquired at a rate of 1Hz throughout the experimental procedure which included a no-drug baseline (10 s duration) and response to 100 μM DHPG (20 s period following drug application). All solutions used during imaging contained standard ACSF and the sodium channel blocker tetrodotoxin (1 μM). Slices received continuous bath and local perfusion of solutions at room temperature throughout the imaging procedure. Drugs

were applied locally via a VC-6M Mini-Valve System-controlled perfusion system (Warner Instruments, Hamden, CT USA). NMDA (500 μM) was applied at the end of each experiment as a positive control for correct placement of local perfusion tube.

Fluo-4 calcium imaging of corticostriatal co-cultured neurons

Corticostriatal co-cultures were prepared from P1 littermate *Sapap3* WT and KO mice. Following decapitation, striatal and cortical tissues were dissected in ice-cold dissection solution containing (in mM): 161 NaCl, 5 KCl, 0.5 $MgSO_4$, 2.9 $CaCl_2$, 5 HEPES, 5.6 D-(+)-glucose and 0.006 phenol red at pH 7.4. Tissue was enzymatically digested for 20 minutes at 37°C in dissection solution which also contained: 0.2 mg/mL L-cysteine, 1mM $CaCl_2$, 0.5 mM EDTA (pH 8), 4,000 units/mL DNAse I from bovine pancreas (all from Sigma-Aldrich) and 10 units/mL papain (Worthington Biochemical Corp), pH 8.0. The digestion was inactivated by removal of the supernatant and addition of dissection solution containing 2.5 mg/mL BSA, 2.5 mg/mL Trypsin inhibitor, and 4,000 units/mL DNAse I from bovine pancreas (all from Sigma-Aldrich). Tissue was triturated with low-resistance, fire-polished Pasteur pipettes, passed through 70 μm cell sieves (BD Biosciences), and pelleted at 200g for 8 minutes before resuspending in serum media that consisted of: Minimum Essential Medium with Earle's Salts without L-glutamine (Sigma-Aldrich), 5% Fetal Bovine Serum, 25 mM Glucose and 0.02% Mito+ Serum Extender (BD Biosciences). Cortical and striatal cells were plated at a 1:1 ratio at a density of 16 – 20 × 10^3 cells/well on Greiner 96 well poly-d-lysine-coated glass bottom plates (Sigma-Aldrich) in 80% Neurobasal A media (NBA) containing 1× B-27 Serum-Free Supplement (Gibco) and 1x Glutamax-1 Supplement (Invitrogen) and 20% serum media.

On the day of imaging (DIV 15 – 17), cultures received a 20% media exchange with NBA containing 100 mM HEPES pH 7.4 and were transferred to the cell imaging facility where they were imaged using the BD Pathway 855 high-content, high-throughput imaging system and an Olympus Plan Fluo 0.75 NA, 20× objective. All experiments were performed at 36–37°C. Cells were loaded with FLIPR dye for one hour by replacing media with 90 μl of filtered imaging buffer containing 1× HANKS (without phenol red or sodium bicarbonate), 4 mM HEPES, 0.5 mg/mL probenecid, 0.1 mg/mL ascorbic acid, 2 μM TTX and 1.5× FLIPR calcium assay kit component A (Invitrogen), pH 7.4. Cells were maintained at 37°C during both dye-loading and imaging. Imaging was completed within one hour following completion of dye loading. Fluorescent images were obtained at 1 Hz during a no-drug baseline (10 s duration), response to 100 μM DHPG (20 s period following drug application) and subsequent response to 1–2 mM NMDA (20 s period), the latter done to identify live neurons.

Calcium dye image analysis—Image processing for both FURA-2AM and FLUO-4 dye experiments was performed using Image J software (http://rsb.info.nih.gov/ij/). For acute slice data, ROIs with a somatic area of 17–53 μm^2 were selected from the tdTomato image (for D1 MSNs) or the EGFP image (for D2 MSNs). For the culture data, somatic regions of interest (ROIs) from MSNs were selected from maximum intensity projections and cell type was confirmed using morphological features observed in the corresponding transmitted light images (somatic diameter ≤ 14 μm and demonstrated somatic circularity of ≥ 0.8). Morphological selection criteria were derived from EGFP-fluorescent cells in striatal cultures prepared from *Drd2*-EGFP transgenic mice.

Fluorescence for all ROIs in both the culture and acute slice was normalized to the mean fluorescence intensity of the ROI during the 10s baseline period preceding application of DHPG and is expressed as the change in fluorescence/mean baseline fluorescence (ΔF/F). Cells were excluded from analysis if they demonstrated an unstable baseline fluorescence

intensity (std. dev. > 0.03 ΔF/F) or showed no positive physiological response to the NMDA application (max response < 0.1 ΔF/F for cultures; <0.15 ΔF/F for acute slices) These objective criteria resulted in exclusion of 10% of WT D1, 9% WT D2, 14% KO D1 and 11% KO D2 cells for the acute slice data. WT and KO culture data were each derived from 13 wells and 3 separate culture preparations. Acute slice data were derived from 7 slices, 3 animals (WT) and 8 slices, 2 animals (KO). Additionally, < 1.5% of transgene positive cells in the acute slices expressed both EGFP and tdTomato and, when present, such cells were excluded from the analysis. Data are represented as the mean maximal response (within 20 seconds after DHPG application) ± SEM. *N* values represent the number of cells per condition.

Immunocytochemistry and image analysis

Corticostriatal co-cultures prepared as described above were used to measure the surface expression of mGluR5. On DIV 13–14, cultures were fixed with 4% paraformaldehyde in 4% sucrose for 15 minutes at room temperature. Cultures were then rinsed with PBS and blocked in PBS with 0.2% gelatin, 2% BSA, 2% glycine and 50 mM NH_4Cl for 30 minutes at room temperature. Cultures were stained with anti-mGluR5 N-terminus rabbit polyclonal antibodies (1:50, Alomone Labs AGC-007) overnight at 4°C. Cultures were then rinsed in PBS and permeabilized in PBS with 0.25% Triton X-100 for 5 minutes at room temperature. Cultures were rinsed with PBS, blocked and then incubated with monoclonal antibodies against rat DARPP-32 (1:40, R&D Systems MAB4230), a marker used to identify MSNs, for 2 hours at room temperature. Cultures were then rinsed and incubated with the appropriate secondary antibodies (Alexa Fluor 568-conjugated goat anti-rabbit IgG, 1:800, Molecular Probes; Cy5-conjugated donkey anti-rat IgG, 1:200, Jackson ImmunoResearch) for 2 hours at room temperature. After final washing with PBS, Fluoromount-G (Southern Biotech) was used to mount coverslips. Surface immunostaining conditions were confirmed by lack of staining with DARPP32 when incubated under non-permeabilizing conditions. Images were collected with a 40x objective on an LSM 510 confocal microscope (Zeiss). Alexa Fluor 568 dye was excited with a 561 nm Diode laser. Cy5 dye was excited with a 633 nm HeNe laser. No crosstalk between channels was detected under these settings. All mGluR5 images were collected under identical acquisition conditions and sub-saturating conditions. Images were collected from three independent batches of cultures with two coverslips per group for each batch. Six images were taken from each coverslip. Two dendritic regions (approx. 40 μm approximate length) were selected for analysis by a separate experimenter who used only the DARPP32-immunostained and transmitted light images for selection. Dendrites were selected if they were clearly part of a cell with high intensity DARPP32 staining (an indicator of medium spiny neurons) and did not have other dendrites overlying. For quantitative analysis, the average mGluR5 immunostaining intensity (total intensity/total area of dendritic region)(arbitrary units/pixel abbreviated a.u./pixel) was measured on DARPP32-positive dendritic regions with MetaMorph software (Molecular Devices). In data not shown, an analysis of total mGluR5 intensity normalized to the total vGluT1 (Synaptic Systems, Cat#135511) intensity in dendritic regions of interest resulted in similar statistically significant conclusions.

Drugs

All drugs were made as concentrated stock solutions and diluted in ACSF to their final concentration on the experiment day. N-(Piperidin-1-yl)-5-(4-iodophenyl)-1-(2,4-dichlorophenyl)-4-methyl-1H-pyrazole-3-carboxamide (AM251), WIN 55212-2, 2-Methyl-6-(phenylethynyl)-pyridine hydrochloride (MPEP), (RS)-3,5-Dihydroxyphenylglycine (DHPG), 3-Cyano-*N*-(1,3-diphenyl-1*H*-pyrazol-5-yl) benzamide (CDPPB), tetrodotoxin citrate (TTX), *N*-Methyl-D-aspartic acid (NMDA) and nifedipine were purchased from Tocris. Picrotoxin and bovine serum albumin (BSA) were purchased

from Sigma. 0.05% BSA was used as a carrier for AM251, WIN 55212-2 and CDPPB experiments and their corresponding vehicle control experiments. For AM251 experiments (Fig. 2), slices were pre-incubated with AM251 for 1 hour prior to recording and continuously perfused with antagonist during recording. All other drug treatments were applied during bath perfusion only.

Statistical analysis

All electrophysiological recording data were analyzed by Clampfit 10.0 software (Axon Instruments, USA). The peak amplitude of field population spikes and evoked ESPCs was measured and data were transferred to Microsoft Excel and GraphPad Prism (GraphPad Software, USA) for analysis and graphing. Data are presented as mean ± s.e.m and the *n* value given for each experiment refers to the number of cells analyzed unless otherwise noted. Bar graph data present the average value of the response during the last 10 min of the 10 s stimulation interval period normalized to the baseline response value. Two-way repeated measures ANOVA (rmANOVA) was performed for the entire time course before post hoc comparisons were made with Student's t-test or Mann-Whitney rank test (JMP8.0 software, SAS institute Inc, USA). The significance level for all tests was $p < 0.05$ (*). For linear regression analysis, R^2 values are reported.

RESULTS

Activity-dependent synaptic depression of striatal excitatory synapses is increased in *Sapap3* KO mice

Abnormal activity-dependent depression in *Sapap3* KO mice was initially suspected because of an observation that evoked extracellular field potentials in *Sapap3* KO striatal slices were preferentially unstable (rundown) or lost. However, stable responses could be obtained for both WT and KO genotypes by reducing the frequency of stimulation, suggesting that rundown of responses in KO brain slices might be caused by activity-dependent synaptic depression. To test this hypothesis, we evaluated the change in field potential population spike (PS) amplitude and PS paired-pulse ratio (PPR) that occurred as a consequence of increasing stimulation rate. Stable baseline PS field potential responses were first obtained in dorsolateral striatum by stimulating each 90 s. Thereafter, the stimulation interval was reduced to 10 s. In response to the reduction in stimulation interval, PS amplitude in *Sapap3* KO slices depressed markedly (PS amplitude relative to baseline – WT, 74 ± 4%, $n = 10$; KO, 43 ± 7%, $n = 14$, $p = 0.003$, *t*-test)(Fig. 1A–C). Concomitantly, the PPR of the PS amplitude increased (PPR relative to baseline - WT, 124 ± 3%, $n = 10$; KO, 182 ± 22%, $n = 14$, $p = 0.038$, *t*-test)(Fig. 1D, E). These findings were also present and of similar magnitude in mature adult mice (8 weeks and older) (PS amplitude relative to baseline – WT, 71 ± 5%, $n=10$, KO, 40 ± 4%, $n =11$, $p= 0.0002$, *t*-test). Although the amplitudes of basal field potential responses were lower in *Sapap3* KO mice than WT mice (baseline PS amplitude – WT, −1.2 ± 0.1 mV, $n = 20$; KO, −0.9 ± 0.1 mV, $n = 25$; $p = 0.035$, *t*-test), there was no correlation between the degree of activity-dependent depression and initial PS amplitude or PPR (% depression vs. initial PS amplitude - WT, $R^2 = 0.077$; KO, $R^2 = 0.0004$; % depression vs. initial PPR - WT, $R^2 = 0.002$; KO, $R^2 = 0.110$).

Because PPR of synaptic responses varies inversely with release probability, the frequency-dependent increase in PPR of *Sapap3* KO PS responses suggests that a decrease in presynaptic release probability may underlie the PS depression. However, PS can also be influenced by non-synaptic contributions. To isolate the synaptic contributions, whole-cell, voltage-clamp recordings were performed. In three week-old mice, whole-cell, voltage-clamp recordings were obtained from defined subpopulations of MSNs based on their expression of BAC transgenes encoding fluorescent reporters, *Drd2*-EGFP ("D2") (Gong et

al., 2003) or *Drd1a*-tdTomato ("D1") (Shuen et al., 2008). These two populations reflect MSNs projecting to the indirect and direct pathways of the basal ganglia, respectively, and have distinct synaptic properties (Kreitzer and Malenka, 2007; Cepeda et al., 2008; Gertler et al., 2008). Using a similar stimulation paradigm, evoked excitatory postsynaptic currents (eEPSCs) in D2 MSNs from *Sapap3* KO mice showed a significant increase in activity-dependent depression relative to D2 MSNs from WT mice (eEPSC amplitude relative to baseline - WT, 53 ± 3%, $n = 13$; KO, 40 ± 2%, $n = 14$; $p = 0.002$, *t*-test)(Fig. 1F–H). Paired-pulse ratios of eEPSCs were also significantly increased in D2 MSNs of *Sapap3* KO mice relative to WT mice (PPR relative to baseline - WT, 113 ± 2%, $n = 13$; KO, 131 ± 5%, $n = 14$; $p = 0.003$, *t*-test) (Fig. 1I, J). In D1 MSNs, qualitatively similar findings were present in *Sapap3* KO mice. However, WT D1 MSNs had a greater degree of activity-dependent depression than WT D2 MSNs in this stimulation paradigm (eEPSC amplitude relative to baseline - D1 WT, 47 ± 3%, $n = 16$; D2 WT, 53 ± 3%, $n = 13$). As a result, smaller increases in synaptic depression and PPR were observed in D1 MSNs of *Sapap3* KO mice compared to WT (eEPSC amplitude relative to baseline - WT, 47 ± 3%, $n = 16$, KO, 39 ± 5%, $n = 12$, $p = 0.138$, rmANOVA; $p = 0.143$, t-test. PPR - WT, 118 ± 5%, $n = 16$, KO, 129 ± 5%, $n = 12$, $p = 0.02$, rmANOVA; $p = 0.117$, t-test). For this reason, in subsequent analyses, we focused on D2 MSNs for whole-cell recording experiments. Together these experiments show that MSN excitatory synapses of *Sapap3* KO mice have increased activity-dependent synaptic depression that is associated with a change in PPR, suggesting a change in release probability.

Excessive synaptic depression at *Sapap3* KO excitatory synapses requires endocannabinoid signaling

It is intriguing to consider that SAPAP3, a postsynaptic protein, may cause enhanced synaptic depression through a presynaptic mechanism. We hypothesized that retrograde signaling by eCBs was involved because abnormalities in eCB signaling could arise from postsynaptic dysfunction and be expressed as a change in presynaptic function. To test this hypothesis, we performed three sets of experiments. First, pre-incubation of striatal slices with AM251 (3 μM), a potent type 1 endocannabinoid receptor (CB1R) antagonist, abolished the genotypic differences in activity-dependent depression of both field potential responses (Fig. 2A–C) and D2 MSN eEPSCs (Fig. 2G–I) between *Sapap3* KO and WT mice. Second, we found that the activity-dependent depression was absent at room temperature (PS amplitude relative to baseline - WT, 99 ± 3%, $n = 6$; KO, 93 ± 6%, $n = 6$; $p = 0.391$, *t*-test) (Fig. 2D). Although temperature may have diverse effects on neurotransmission, these data are consistent with a role for eCBs because, in the striatum, room temperature can inhibit eCB-mediated synaptic depression (Kreitzer and Malenka, 2005; Adermark and Lovinger, 2007; Adermark et al., 2009), presumably due to decreased activity of the plasma membrane transporter required for the extracellular transport of eCBs (Beltramo et al., 1997; Hillard and Jarrahian, 2000; Ronesi et al., 2004; Adermark and Lovinger, 2007; Hillard et al., 2007). Third, genetic deletion of *CB1R* significantly decreased striatal activity-dependent depression and PPR changes in *Sapap3* KO mice to levels that were no longer distinguishable from *Sapap3* WT mice (PS amplitude relative to baseline – *Sapap*3 KO/CB1R KO, 81 ± 6%, $n = 11$, WT, 74 ± 4%, $n = 10$, $p = 0.364$; PS PPR relative to baseline – *Sapap*3 KO/CB1R KO, 120 ± 4%, $n = 11$, WT, 124 ± 3%, $n = 10$, $p = 0.357$)(Fig. 2E, 2F, 1B, 1D). Thus, altogether three lines of evidence show that eCB signaling mediates the excessive depression of MSN excitatory synapses in *Sapap3* KO mice.

To investigate whether signaling through CB1Rs was altered in *Sapap3* KO MSNs, CB1Rs were directly activated with agonist, WIN 55212-2. At concentrations eliciting sub-maximal levels of synaptic depression, WIN 55212-2 (1 μM) similarly depressed eEPSCs (eEPSC

amplitude relative to baseline – WT: 69 ± 4%, n=10, KO, 69 ± 2%, n=14, $p = 0.970$, *t*-test) (Fig. 2J) and increased PPR in WT and KO MSNs (PPR relative to baseline – WT: 116 ± 3%, $n = 10$, KO, 120 ± 6%, $n = 14$, $p = 0.559$, *t*-test). Therefore, although CB1Rs are required for the activity-dependent depression, we found no evidence for an alteration in CB1R signaling itself in *Sapap3* KO mice.

Sapap3 KO MSNs engage endocannabinoid signaling under anomalous conditions

When eCB signaling is blocked, a degree of synaptic depression persists in both genotypes (Fig. 2B, E, H). Therefore, we investigated the degree of synaptic depression that is mediated by eCBs in each genotype by comparing depression in the absence and presence of AM251 within genotypes. At WT striatal excitatory synapses, AM251 does not alter the degree of eEPSC depression (Fig. 2K) indicating that eCB-mediated synaptic depression is not normally engaged under these conditions. By contrast, an AM251-sensitive component of synaptic depression was readily observed at striatal excitatory synapses lacking SAPAP3 (Fig. 2L). Furthermore, the eCB-independent component of depression is similar in KO and WT MSNs (Fig. 1, 2). These findings reveal that loss of SAPAP3 engages eCB-mediated synaptic plasticity when it is not normally expressed.

Anomalous endocannabinoid synaptic plasticity at *Sapap3* KO synapses requires mGluR5 activity

Because we observed eCB-mediated synaptic plasticity under anomalous conditions in *Sapap3* KO mice, we evaluated whether the upstream signaling events that are normally required for eCB activity at striatal excitatory synapses were also required in this aberrant context. Endocannabinoid-mediated long-term depression (LTD) is a well-described form of eCB-mediated synaptic plasticity at striatal MSN excitatory synapses. Striatal eCB-LTD requires both L-type voltage gated calcium channels (VGCC) and group 1 mGluRs (Calabresi et al., 1994; Sung et al., 2001; Kreitzer and Malenka, 2005; Wang et al., 2006). Short-term eCB-mediated synaptic plasticity as a result of afferent axonal stimulation alone has not been described at these synapses. However, these synapses do appear to be capable of short-term eCB-mediated synaptic plasticity if GPCRs critical for triggering endocannabinoid release, such as group 1 mGluRs, are pharmacologically stimulated (Kreitzer and Malenka, 2005; Narushima et al., 2006; Yin and Lovinger, 2006).

In *Sapap3* KO MSNs, the mGluR5 antagonist, MPEP (40 μM) significantly reduced the degree of activity-dependent synaptic depression and PPR increase (Fig. 3A, B). Levels of activity-dependent synaptic depression and PPR in MPEP-treated *Sapap3* KO mice were indistinguishable from WT mice (Fig. 3C, D). By contrast, the L-type calcium channel antagonist, nifedipine (10 μM), had no effect on synaptic depression or PPR at *Sapap3* KO D2 MSNs (Fig. 3E, F). These results indicate that the anomalous eCB-mediated plasticity of *Sapap3* KO striatal excitatory synapses requires signaling by mGluR5.

Group 1 mGluR signaling and mGluR5 surface expression are increased in MSNs of *Sapap3* KO mice

Because mGluR5 activity is required for the abnormal synaptic depression in *Sapap3* KO mice and SAPAP3 might alter group 1 mGluR activity by virtue of its biochemical interaction with Shank, a protein found in a complex with group 1 mGluRs (Tu et al., 1999; Sala et al., 2001; Hwang et al., 2005), we investigated whether *Sapap3* deletion altered the activity of group I mGluRs. Activity of these receptors was monitored by measuring changes in intracellular calcium levels in response to application of DHPG, a non-selective group 1 mGluR agonist. Group 1 mGluRs are coupled to $G\alpha_{q/11}$-type G proteins that increase cytosolic calcium when activated as a consequence of phospholipase C activation and inositol-1,4,5-trisphosphate (IP_3) production. In this assay, DHPG (100 μM) was

applied to acute striatal brain slices expressing fluorescent reporters to differentiate D1 and D2 MSNs and in the presence of tetrodotoxin to prevent action potentials. Intracellular calcium levels were monitored in the somata of striatal MSNs using the calcium indicator dye, FURA2-AM and 2-photon microscopic imaging. In response to DHPG, both D1 and D2 MSNs from *Sapap3* KO mice had larger calcium transients compared to WT MSNs (Fig. 4).

We next investigated whether surface levels of group 1 mGluRs were also altered by *Sapap3* deletion. Immunocytochemical methods were used to measure mGluR5 surface levels on dendrites of striatal neurons (indicated by high intensity DARPP32 immunostaining) in corticostriatal co-cultures. We first confirmed that the cultured striatal neurons from *Sapap3* KO mice faithfully reproduced the intracellular calcium signaling abnormality in response to DHPG that was observed in acute brain slice MSNs (Fig. 5A, B). Using this culture preparation, the average mGluR5 immunostaining intensity for a given dendritic region was measured. The average intensity of mGluR5 immunostaining on DARPP32-positive dendrites was significantly increased in *Sapap3* KO neurons as compared to WT (WT, 10 ± 0.8 a.u./pixel, $n = 71$ dendritic regions; KO, 14 ± 1 a.u./pixel, $n = 75$ dendritic regions; $p = 0.003$, Mann-Whitney) (Fig. 5C, D). Analysis of the distribution of average mGluR5 intensities over the population of dendrites examined in each group further revealed that a uniform rightward shift was responsible for this increase, rather than a discrete change in a subpopulation of dendrites (Fig. 5E).

Enhancing synaptic mGluR5 activity at WT synapses increases activity-dependent depression

Thus far, our results suggest that an increase in the number and/or activity of type 5 mGluRs may underlie the enhanced eCB-mediated synaptic plasticity observed at MSN excitatory synapses of *Sapap3* KO mice. To directly test this possibility, we examined the role of mGluR5 activation in this process. If increased activation of mGluR5 was responsible for triggering eCB-mediated synaptic depression in *Sapap3* KO mice, increasing the number of activated type 5 mGluRs at WT synapses might be sufficient to reproduce the KO phenotype. Likewise, the same manipulation might be occluded at KO synapses.

To selectively increase the activity of only those mGluRs that are endogenously exposed to glutamate upon synaptic stimulation, the positive allosteric modulator of mGluR5, CDPPB was used (Lindsley et al., 2004; Kinney et al., 2005). In the activity-dependent stimulation paradigm, potentiation of synaptically activated mGluR5 by CDPPB increased the level of WT synaptic depression to that of KO synapses (WT+CDPPB, 55 ± 8%, $n = 8$; KO +CDPPB, 53 ± 5%, $n = 10$, $p = 0.836$, t-test; WT + CDPPB (Fig. 6B) vs. KO (Fig. 1C), $p = 0.328$, *t*-test)(Fig. 6A, B). By contrast, at KO synapses, CDPPB did not increase depression (KO + CDPPB (Fig. 6B) vs. KO (Fig. 1C), $p = 0.350$, *t*-test). Similar effects on field PS PPR were observed (Fig. 6C, D). These results demonstrate that, in WT mice, enhanced mGluR5 activation is sufficient to reproduce the degree of activity-dependent depression observed in KO mice. In addition, KO synapses do not express further activity-dependent depression with CDPPB, suggesting that the anomalous depression in KO synapses is due to enhanced mGluR5 activity.

Anomalous endocannabinoid signaling at *Sapap3* KO striatal excitatory synapses produces short-term eCB plasticity

To investigate whether the 90s/10s interval activity-dependent depression protocol resulted in short- or long-lasting synaptic depression of KO synapses, we performed two experiments. First, after 20 minutes of paired stimulation at 10 s intervals, AM251 was capable of reversing the depression and PPR changes of *Sapap3* KO synapses to levels

indistinguishable from WT (Fig. 7A, B). Second, when electrical stimulation was paused briefly (10 min) and resumed at the reduced rate of each 90 s interval, synaptic responses returned to basal values (100 ± 7% of baseline, $n = 5$, $p = 0.963$, *t*-test compared with initial baseline) (Fig. 7C). These two experimental paradigms indicate that the anomalous eCB-mediated synaptic plasticity observed in *Sapap3* KO synapses is a form of short-term plasticity. Short-term eCB-mediated synaptic plasticity in the absence of pharmacological stimulation of G-protein coupled receptors (GPCR) has not been reported at these synapses. Thus, *Sapap3* deletion alters the conditions required for engaging eCB-mediated synaptic depression.

To test whether *Sapap3* deletion alters the magnitude of eCB-mediated synaptic depression, we induced eCB long-term depression (LTD), a readily observed form of eCB synaptic plasticity at D2 MSN excitatory synapses. Endocannabinoid LTD was induced by a commonly used protocol, delivering 4 high-frequency stimulation trains paired with postsynaptic depolarization (Choi and Lovinger, 1997; Kreitzer and Malenka, 2005; Wang et al., 2006). No differences in the magnitude of LTD were observed between genotypes (eEPSC amplitude relative to baseline - WT, 54 ± 7%, $n = 6$; KO, 57 ± 6%, $n = 6$; $p = 0.723$, *t*-test) (Fig. 7D). Thus, although *Sapap3* deletion alters the conditions for engaging eCB-mediated synaptic depression, we did not find evidence that *Sapap3* deletion alters the magnitude of such depression once engaged (Fig. 6A, B, 7D).

DISCUSSION

In the brain, mGluR-dependent endocannabinoid signaling is a common mechanism for activity-dependent regulation of synaptic strength. Although the pathway stimulating the synthesis of endocannabinoids has been well studied (Kano et al., 2009), little is known about postsynaptic mechanisms regulating the induction of this pathway. Here, we investigate excitatory synaptic transmission of striatal MSNs in *Sapap3* KO mice and identify a role for SAPAPs in regulating the induction of eCB-mediated synaptic plasticity. Our results indicate that the normal role of SAPAPs is to negatively regulate mGluR5 activity and thereby restrict the conditions under which eCB-mediated synaptic depression occurs (see model Fig. 7E). These results identify SAPAPs for the first-time as potential mediators of endocannabinoid metaplasticity and further suggest that altered mGluR and/or eCB signaling may contribute to the pathological OCD-like behaviors of *Sapap3* mutant mice.

Loss of SAPAP3 promotes eCB-mediated synaptic plasticity at MSN excitatory synapses

Endocannabinoids mediate diverse forms of synaptic plasticity throughout the nervous system. Conditions for the induction and expression of eCB-mediated synaptic plasticity can vary among circuits and between activity states (reviewed in Wilson and Nicoll, 2002; Heifets and Castillo, 2009; Kano et al., 2009; Lovinger, 2010). Presynaptic factors have been identified that can influence whether short- or long-term inhibition of presynaptic release occurs as a consequence of CB1R activation (Ronesi et al., 2004; Chevaleyre et al., 2007; Singla et al., 2007). Although there is also evidence that postsynaptic mechanisms are at play, little is known about specific postsynaptic molecules that regulate eCB-mediated synaptic plasticity (Edwards et al., 2008; Kim and Alger, 2010; Roloff et al., 2010). In the present study, we observe that excitatory striatal synapses of *Sapap3* KO mice engage eCB signaling under conditions that are not normally sufficient to elicit eCB-mediated synaptic depression. Although both genotypes exhibit synaptic depression under the activity-dependent protocol, only *Sapap3* KO mice express an eCB-dependent component. Our results further provide evidence that (1) there is a threshold level of mGluR activation that is required to trigger eCB-mediated synaptic depression, (2) KO synapses reach threshold under conditions that WT synapses do not, and (3) once eCB-mediated synaptic depression

is triggered, there are not additional significant differences in the magnitude of the effect at KO synapses in comparison to WT synapses. These results indicate that SAPAP3 may primarily influence the context under which eCB-mediated synaptic depression is activated. In this study, we show that genetic deletion of *Sapap3* lowers the threshold for activating eCB-mediated synaptic plasticity by increasing mGluR activity. In future studies, it will be of interest to determine how SAPAP3 activity is modulated in space and time to regulate mGluR activity and eCB-mediated synaptic plasticity.

Loss of SAPAP3 increases group 1 mGluR activity and mGluR5 cell surface expression

Group 1 mGluRs are known triggers for eCB synthesis (Maejima et al., 2001; Varma et al., 2001; Ohno-Shosaku et al., 2002). In Sapap3 KO neurons, we observe both a functional increase in group 1 mGluR activity (intracellular calcium transients in response to DHPG) and a physical increase in mGluR5 surface receptors. These findings provide a mechanism for increased eCB-mediated synaptic plasticity at *Sapap3* KO synapses. Although it is logical to speculate that the increased surface receptors are responsible for the increased mGluR activity, our data do not exclude the possibility that mGluR activation or coupling to downstream signaling events is enhanced independent of the increase in surface receptors. Such changes in group 1 mGluR activity have been reported when mGluR scaffolding is altered (Ango et al., 2001; Sala et al., 2005; Kammermeier and Worley, 2007). Likewise, although most of the experiments specifically evaluate mGluR5, the predominant group 1 mGluR expressed in MSNs, we cannot exclude the possibility that *Sapap3* deletion also increases mGluR1 activity. Our findings of enhanced group 1 mGluR activity in *Sapap3* KO mice indicate that other downstream sequelae of group 1 mGluR activation may also be altered.

One potential mechanism for the increase in surface mGluR5 in *Sapap3* KO mice is through an impairment of mGluR endocytosis. This possibility is supported by prior studies that implicate Homer proteins in receptor endocytosis and localization of endocytic zones to dendritic spines (Gray et al., 2003; Davidkova and Carroll, 2007; Lu et al., 2007; Petrini et al., 2009). Homer proteins form a ternary complex with SAPAP3 and Shank3, providing a biochemical basis by which loss of SAPAP3 could alter Homer activity (Tu et al., 1999; Sala et al., 2001). A specific role for Homer in regulating group 1 mGluR endocytosis and surface levels has been demonstrated in experiments over-expressing Homer 1a, a short form of Homer that disrupts the interaction of long forms of Homer proteins with other scaffold proteins (Minami et al., 2003). Several recent studies demonstrate that Homer proteins can also alter group 1 mGluR-dependent endocannabinoid signaling (Fourgeaud et al., 2004; Jung et al., 2007; Roloff et al., 2010). Together these findings suggest that Shank and Homer may be functionally important in mediating the effects of SAPAP3 on group 1 mGluRs and endocannabinoids. Further experiments directly testing the role of these protein interactions are necessary.

Intriguingly, two clinical disorders that share a core feature of compulsive-repetitive behaviors, autism and Fragile X mental retardation, might also disrupt signaling through a putative mGluR/Homer/Shank/SAPAP pathway. *Shank3* mutation is associated with a form of autism (Durand et al., 2007). Shank proteins interact biochemically with SAPAP and Homer (Tu et al., 1999). In mouse models for Fragile X mental retardation, SAPAP3 levels are altered (Narayanan et al., 2008) and both excessive group 1 mGluR and endocannabinoid activity have been reported (Huber et al., 2002; Bear et al., 2004; Maccarrone et al., 2010; Zhang and Alger, 2010). These behavioral and molecular similarities with *Sapap3* KO mice suggest that increased mGluR5 activity and/or eCB-mediated synaptic plasticity in the striatum may represent a common mechanism for the expression of compulsive-repetitive behaviors.

Acknowledgments

Grant support for this work was provided by National Institute of Neurological Disorders and Stroke (T32NS051156 [K.A.], NS064577 [N.C.], NS054840 [N.C.]), Tourette Syndrome Association, Klingenstein Foundation and NARSAD to N.C., National Institute of Mental Health (F32MH084460 [J.T.], MH081201 [G.F.]) and The Simons Foundation Autism Research Initiative (SFARI) and The Hartwell Foundation to G.F. We gratefully acknowledge Samantha Tracy, David Pan and Audrey Nelson for outstanding technical assistance, members of the Calakos lab for critical discussions, Serena Dudek and Ben Philpot for comments on the manuscript, Rui Costa and Andreas Zimmer for providing *CB1R* KO mice, and Bryan Roth, Noah Sciaky and John Allen for critical support in BD Pathway imaging experiments.

References

Adermark L, Lovinger DM. Retrograde endocannabinoid signaling at striatal synapses requires a regulated postsynaptic release step. Proc Natl Acad Sci U S A. 2007; 104:20564–20569. [PubMed: 18077376]

Adermark L, Talani G, Lovinger DM. Endocannabinoid-dependent plasticity at GABAergic and glutamatergic synapses in the striatum is regulated by synaptic activity. Eur J Neurosci. 2009; 29:32–41. [PubMed: 19120438]

Ango F, Prezeau L, Muller T, Tu JC, Xiao B, Worley PF, Pin JP, Bockaert J, Fagni L. Agonist-independent activation of metabotropic glutamate receptors by the intracellular protein Homer. Nature. 2001; 411:962–965. [PubMed: 11418862]

Bear MF, Huber KM, Warren ST. The mGluR theory of fragile X mental retardation. Trends Neurosci. 2004; 27:370–377. [PubMed: 15219735]

Beltramo M, Stella N, Calignano A, Lin SY, Makriyannis A, Piomelli D. Functional role of high-affinity anandamide transport, as revealed by selective inhibition. Science. 1997; 277:1094–1097. [PubMed: 9262477]

Boeckers TM, Winter C, Smalla KH, Kreutz MR, Bockmann J, Seidenbecher C, Garner CC, Gundelfinger ED. Proline-rich synapse-associated proteins ProSAP1 and ProSAP2 interact with synaptic proteins of the SAPAP/GKAP family. Biochem Biophys Res Commun. 1999; 264:247–252. [PubMed: 10527873]

Calabresi P, Pisani A, Mercuri NB, Bernardi G. Post-receptor mechanisms underlying striatal long-term depression. J Neurosci. 1994; 14:4871–4881. [PubMed: 8046457]

Cepeda C, Andre VM, Yamazaki I, Wu N, Kleiman-Weiner M, Levine MS. Differential electrophysiological properties of dopamine D1 and D2 receptor-containing striatal medium-sized spiny neurons. Eur J Neurosci. 2008; 27:671–682. [PubMed: 18279319]

Chevaleyre V, Heifets BD, Kaeser PS, Sudhof TC, Purpura DP, Castillo PE. Endocannabinoid-Mediated Long-Term Plasticity Requires cAMP/PKA Signaling and RIM1alpha. Neuron. 2007; 54:801–812. [PubMed: 17553427]

Choi S, Lovinger DM. Decreased probability of neurotransmitter release underlies striatal long-term depression and postnatal development of corticostriatal synapses. Proc Natl Acad Sci U S A. 1997; 94:2665–2670. [PubMed: 9122253]

Davidkova G, Carroll RC. Characterization of the role of microtubule-associated protein 1B in metabotropic glutamate receptor-mediated endocytosis of AMPA receptors in hippocampus. J Neurosci. 2007; 27:13273–13278. [PubMed: 18045921]

Durand CM, et al. Mutations in the gene encoding the synaptic scaffolding protein SHANK3 are associated with autism spectrum disorders. Nat Genet. 2007; 39:25–27. [PubMed: 17173049]

Edwards DA, Zhang L, Alger BE. Metaplastic control of the endocannabinoid system at inhibitory synapses in hippocampus. Proc Natl Acad Sci U S A. 2008; 105:8142–8147. [PubMed: 18523004]

Fourgeaud L, Mato S, Bouchet D, Hemar A, Worley PF, Manzoni OJ. A single in vivo exposure to cocaine abolishes endocannabinoid-mediated long-term depression in the nucleus accumbens. J Neurosci. 2004; 24:6939–6945. [PubMed: 15295029]

Gertler TS, Chan CS, Surmeier DJ. Dichotomous anatomical properties of adult striatal medium spiny neurons. J Neurosci. 2008; 28:10814–10824. [PubMed: 18945889]

Gong S, Zheng C, Doughty ML, Losos K, Didkovsky N, Schambra UB, Nowak NJ, Joyner A, Leblanc G, Hatten ME, Heintz N. A gene expression atlas of the central nervous system based on bacterial artificial chromosomes. Nature. 2003; 425:917–925. [PubMed: 14586460]

Gray NW, Fourgeaud L, Huang B, Chen J, Cao H, Oswald BJ, Hemar A, McNiven MA. Dynamin 3 is a component of the postsynapse, where it interacts with mGluR5 and Homer. Curr Biol. 2003; 13:510–515. [PubMed: 12646135]

Heifets BD, Castillo PE. Endocannabinoid signaling and long-term synaptic plasticity. Annu Rev Physiol. 2009; 71:283–306. [PubMed: 19575681]

Hillard CJ, Jarrahian A. The movement of N-arachidonoylethanolamine (anandamide) across cellular membranes. Chem Phys Lipids. 2000; 108:123–134. [PubMed: 11106786]

Hillard CJ, Shi L, Tuniki VR, Falck JR, Campbell WB. Studies of anandamide accumulation inhibitors in cerebellar granule neurons: comparison to inhibition of fatty acid amide hydrolase. J Mol Neurosci. 2007; 33:18–24. [PubMed: 17901541]

Hirao K, Hata Y, Deguchi M, Yao I, Ogura M, Rokukawa C, Kawabe H, Mizoguchi A, Takai Y. Association of synapse-associated protein 90/postsynaptic density-95-associated protein (SAPAP) with neurofilaments. Genes Cells. 2000; 5:203–210. [PubMed: 10759891]

Huber KM, Gallagher SM, Warren ST, Bear MF. Altered synaptic plasticity in a mouse model of fragile X mental retardation. Proc Natl Acad Sci U S A. 2002; 99:7746–7750. [PubMed: 12032354]

Hwang JI, Kim HS, Lee JR, Kim E, Ryu SH, Suh PG. The interaction of phospholipase C-beta3 with Shank2 regulates mGluR-mediated calcium signal. J Biol Chem. 2005; 280:12467–12473. [PubMed: 15632121]

Jung KM, Astarita G, Zhu C, Wallace M, Mackie K, Piomelli D. A key role for diacylglycerol lipase-alpha in metabotropic glutamate receptor-dependent endocannabinoid mobilization. Mol Pharmacol. 2007; 72:612–621. [PubMed: 17584991]

Kammermeier PJ, Worley PF. Homer 1a uncouples metabotropic glutamate receptor 5 from postsynaptic effectors. Proc Natl Acad Sci U S A. 2007; 104:6055–6060. [PubMed: 17389377]

Kano M, Ohno-Shosaku T, Hashimotodani Y, Uchigashima M, Watanabe M. Endocannabinoid-mediated control of synaptic transmission. Physiol Rev. 2009; 89:309–380. [PubMed: 19126760]

Kim E, Sheng M. PDZ domain proteins of synapses. Nat Rev Neurosci. 2004; 5:771–781. [PubMed: 15378037]

Kim E, Naisbitt S, Hsueh YP, Rao A, Rothschild A, Craig AM, Sheng M. GKAP, a novel synaptic protein that interacts with the guanylate kinase-like domain of the PSD-95/SAP90 family of channel clustering molecules. J Cell Biol. 1997; 136:669–678. [PubMed: 9024696]

Kim J, Alger BE. Reduction in endocannabinoid tone is a homeostatic mechanism for specific inhibitory synapses. Nat Neurosci. 2010; 13:592–600. [PubMed: 20348918]

Kindler S, Rehbein M, Classen B, Richter D, Bockers TM. Distinct spatiotemporal expression of SAPAP transcripts in the developing rat brain: a novel dendritically localized mRNA. Brain Res Mol Brain Res. 2004; 126:14–21. [PubMed: 15207911]

Kinney GG, O'Brien JA, Lemaire W, Burno M, Bickel DJ, Clements MK, Chen TB, Wisnoski DD, Lindsley CW, Tiller PR, Smith S, Jacobson MA, Sur C, Duggan ME, Pettibone DJ, Conn PJ, Williams DL Jr. A novel selective positive allosteric modulator of metabotropic glutamate receptor subtype 5 has in vivo activity and antipsychotic-like effects in rat behavioral models. J Pharmacol Exp Ther. 2005; 313:199–206. [PubMed: 15608073]

Kreitzer AC, Malenka RC. Dopamine modulation of state-dependent endocannabinoid release and long-term depression in the striatum. J Neurosci. 2005; 25:10537–10545. [PubMed: 16280591]

Kreitzer AC, Malenka RC. Endocannabinoid-mediated rescue of striatal LTD and motor deficits in Parkinson's disease models. Nature. 2007; 445:643–647. [PubMed: 17287809]

Lindsley CW, Wisnoski DD, Leister WH, O'Brien JA, Lemaire W, Williams DL Jr, Burno M, Sur C, Kinney GG, Pettibone DJ, Tiller PR, Smith S, Duggan ME, Hartman GD, Conn PJ, Huff JR. Discovery of positive allosteric modulators for the metabotropic glutamate receptor subtype 5 from a series of N-(1,3-diphenyl-1H- pyrazol-5-yl)benzamides that potentiate receptor function in vivo. J Med Chem. 2004; 47:5825–5828. [PubMed: 15537338]

Lovinger DM. Neurotransmitter roles in synaptic modulation, plasticity and learning in the dorsal striatum. Neuropharmacology. 2010; 58:951–961. [PubMed: 20096294]

Lovinger DM, McCool BA. Metabotropic glutamate receptor-mediated presynaptic depression at corticostriatal synapses involves mGLuR2 or 3. J Neurophysiol. 1995; 73:1076–1083. [PubMed: 7608756]

Lu J, Helton TD, Blanpied TA, Racz B, Newpher TM, Weinberg RJ, Ehlers MD. Postsynaptic positioning of endocytic zones and AMPA receptor cycling by physical coupling of dynamin-3 to Homer. Neuron. 2007; 55:874–889. [PubMed: 17880892]

Maccarrone M, Rossi S, Bari M, De Chiara V, Rapino C, Musella A, Bernardi G, Bagni C, Centonze D. Abnormal mGlu 5 Receptor/Endocannabinoid Coupling in Mice Lacking FMRP and BC1 RNA. Neuropsychopharmacology. 2010; 35:1500–1509. [PubMed: 20393458]

MacLean JN, Yuste R. Imaging action potentials with calcium indicators. Cold Spring Harb Protoc 2009. 2009 pdb prot5316.

Maejima T, Hashimoto K, Yoshida T, Aiba A, Kano M. Presynaptic inhibition caused by retrograde signal from metabotropic glutamate to cannabinoid receptors. Neuron. 2001; 31:463–475. [PubMed: 11516402]

Minami I, Kengaku M, Smitt PS, Shigemoto R, Hirano T. Long-term potentiation of mGluR1 activity by depolarization-induced Homer1a in mouse cerebellar Purkinje neurons. Eur J Neurosci. 2003; 17:1023–1032. [PubMed: 12653978]

Naisbitt S, Kim E, Weinberg RJ, Rao A, Yang FC, Craig AM, Sheng M. Characterization of guanylate kinase-associated protein, a postsynaptic density protein at excitatory synapses that interacts directly with postsynaptic density-95/synapse-associated protein 90. J Neurosci. 1997; 17:5687–5696. [PubMed: 9221768]

Narayanan U, Nalavadi V, Nakamoto M, Thomas G, Ceman S, Bassell GJ, Warren ST. S6K1 phosphorylates and regulates fragile X mental retardation protein (FMRP) with the neuronal protein synthesis-dependent mammalian target of rapamycin (mTOR) signaling cascade. J Biol Chem. 2008; 283:18478–18482. [PubMed: 18474609]

Narushima M, Hashimoto K, Kano M. Endocannabinoid-mediated short-term suppression of excitatory synaptic transmission to medium spiny neurons in the striatum. Neurosci Res. 2006; 54:159–164. [PubMed: 16413076]

Nikolenko V, Watson BO, Araya R, Woodruff A, Peterka DS, Yuste R. SLM Microscopy: Scanless Two-Photon Imaging and Photostimulation with Spatial Light Modulators. Front Neural Circuits. 2008; 2:5. [PubMed: 19129923]

Ohno-Shosaku T, Shosaku J, Tsubokawa H, Kano M. Cooperative endocannabinoid production by neuronal depolarization and group I metabotropic glutamate receptor activation. Eur J Neurosci. 2002; 15:953–961. [PubMed: 11918654]

Petrini EM, Lu J, Cognet L, Lounis B, Ehlers MD, Choquet D. Endocytic trafficking and recycling maintain a pool of mobile surface AMPA receptors required for synaptic potentiation. Neuron. 2009; 63:92–105. [PubMed: 19607795]

Roloff AM, Anderson GR, Martemyanov KA, Thayer SA. Homer 1a gates the induction mechanism for endocannabinoid-mediated synaptic plasticity. J Neurosci. 2010; 30:3072–3081. [PubMed: 20181604]

Romorini S, Piccoli G, Jiang M, Grossano P, Tonna N, Passafaro M, Zhang M, Sala C. A functional role of postsynaptic density-95-guanylate kinase-associated protein complex in regulating Shank assembly and stability to synapses. J Neurosci. 2004; 24:9391–9404. [PubMed: 15496675]

Ronesi J, Gerdeman GL, Lovinger DM. Disruption of endocannabinoid release and striatal long-term depression by postsynaptic blockade of endocannabinoid membrane transport. J Neurosci. 2004; 24:1673–1679. [PubMed: 14973237]

Rumbaugh G, Sia GM, Garner CC, Huganir RL. Synapse-associated protein-97 isoform-specific regulation of surface AMPA receptors and synaptic function in cultured neurons. J Neurosci. 2003; 23:4567–4576. [PubMed: 12805297]

Sala C, Roussignol G, Meldolesi J, Fagni L. Key role of the postsynaptic density scaffold proteins shank and homer in the functional architecture of Ca2+ homeostasis at dendritic spines in hippocampal neurons. J Neurosci. 2005; 25:4587–4592. [PubMed: 15872106]

Sala C, Piech V, Wilson NR, Passafaro M, Liu GS, Sheng M. Regulation of dendritic spine morphology and synaptic function by Shank and Homer. Neuron. 2001; 31:115–130. [PubMed: 11498055]

Sheng M, Pak DT. Glutamate receptor anchoring proteins and the molecular organization of excitatory synapses. Ann N Y Acad Sci. 1999; 868:483–493. [PubMed: 10414325]

Shuen JA, Chen M, Gloss B, Calakos N. Drd1a-tdTomato BAC transgenic mice for simultaneous visualization of medium spiny neurons in the direct and indirect pathways of the basal ganglia. J Neurosci. 2008; 28:2681–2685. [PubMed: 18337395]

Singla S, Kreitzer AC, Malenka RC. Mechanisms for synapse specificity during striatal long-term depression. J Neurosci. 2007; 27:5260–5264. [PubMed: 17494712]

Sung KW, Choi S, Lovinger DM. Activation of group I mGluRs is necessary for induction of long-term depression at striatal synapses. J Neurophysiol. 2001; 86:2405–2412. [PubMed: 11698530]

Takeuchi M, Hata Y, Hirao K, Toyoda A, Irie M, Takai Y. SAPAPs. A family of PSD-95/SAP90-associated proteins localized at postsynaptic density. J Biol Chem. 1997; 272:11943–11951. [PubMed: 9115257]

Tu JC, Xiao B, Naisbitt S, Yuan JP, Petralia RS, Brakeman P, Doan A, Aakalu VK, Lanahan AA, Sheng M, Worley PF. Coupling of mGluR/Homer and PSD-95 complexes by the Shank family of postsynaptic density proteins. Neuron. 1999; 23:583–592. [PubMed: 10433269]

Valtschanoff JG, Weinberg RJ. Laminar organization of the NMDA receptor complex within the postsynaptic density. J Neurosci. 2001; 21:1211–1217. [PubMed: 11160391]

Varma N, Carlson GC, Ledent C, Alger BE. Metabotropic glutamate receptors drive the endocannabinoid system in hippocampus. J Neurosci. 2001; 21:RC188. [PubMed: 11734603]

Wang Z, Kai L, Day M, Ronesi J, Yin HH, Ding J, Tkatch T, Lovinger DM, Surmeier DJ. Dopaminergic control of corticostriatal long-term synaptic depression in medium spiny neurons is mediated by cholinergic interneurons. Neuron. 2006; 50:443–452. [PubMed: 16675398]

Welch JM, Wang D, Feng G. Differential mRNA expression and protein localization of the SAP90/PSD-95-associated proteins (SAPAPs) in the nervous system of the mouse. J Comp Neurol. 2004; 472:24–39. [PubMed: 15024750]

Welch JM, Lu J, Rodriguiz RM, Trotta NC, Peca J, Ding JD, Feliciano C, Chen M, Adams JP, Luo J, Dudek SM, Weinberg RJ, Calakos N, Wetsel WC, Feng G. Cortico-striatal synaptic defects and OCD-like behaviours in Sapap3-mutant mice. Nature. 2007; 448:894–900. [PubMed: 17713528]

Wilson RI, Nicoll RA. Endocannabinoid signaling in the brain. Science. 2002; 296:678–682. [PubMed: 11976437]

Wokosin DL, Loughrey CM, Smith GL. Characterization of a range of fura dyes with two-photon excitation. Biophys J. 2004; 86:1726–1738. [PubMed: 14990500]

Yin HH, Lovinger DM. Frequency-specific and D2 receptor-mediated inhibition of glutamate release by retrograde endocannabinoid signaling. Proc Natl Acad Sci U S A. 2006; 103:8251–8256. [PubMed: 16698932]

Zhang L, Alger BE. Enhanced endocannabinoid signaling elevates neuronal excitability in fragile X syndrome. J Neurosci. 2010; 30:5724–5729. [PubMed: 20410124]

Zimmer A, Zimmer AM, Hohmann AG, Herkenham M, Bonner TI. Increased mortality, hypoactivity, and hypoalgesia in cannabinoid CB1 receptor knockout mice. Proc Natl Acad Sci U S A. 1999; 96:5780–5785. [PubMed: 10318961]

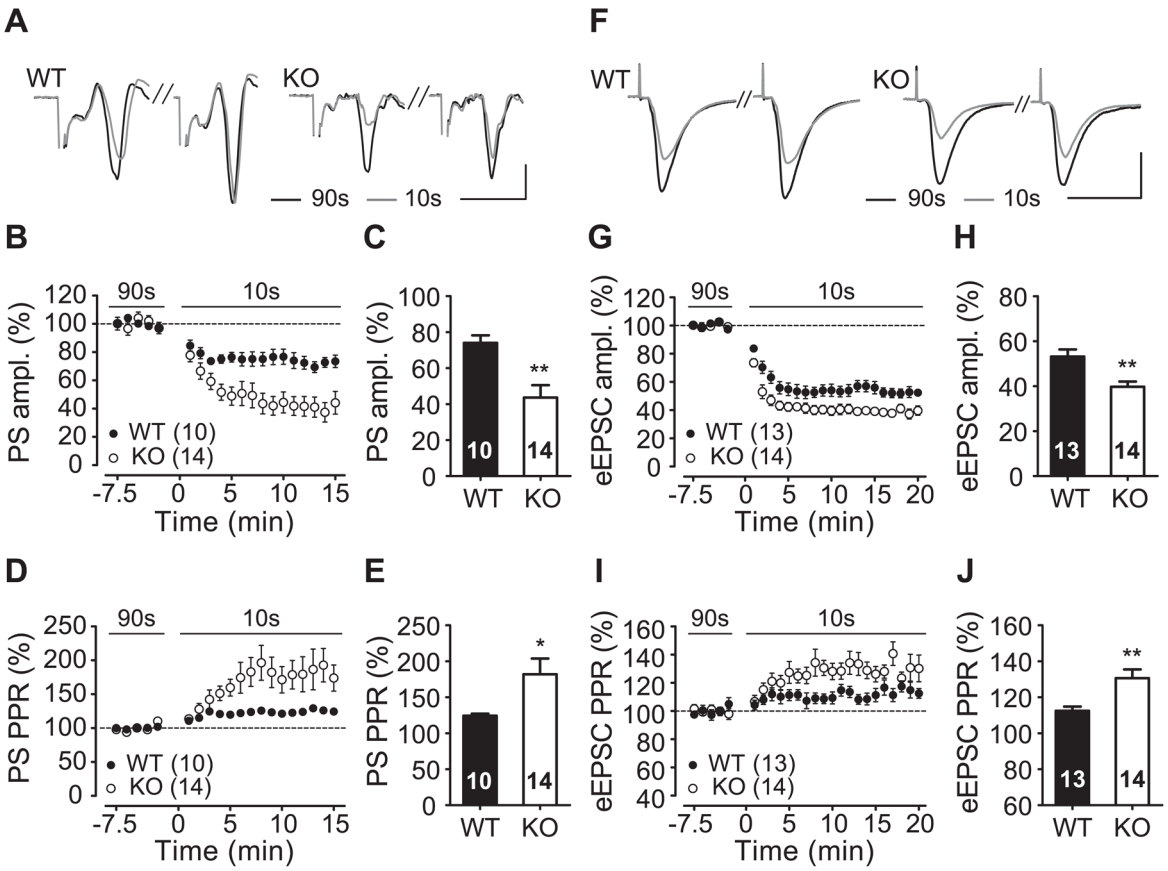

Figure 1. Activity-dependent synaptic depression of MSN excitatory synapses is enhanced in *Sapap3* KO mice

A–E, A decrease in stimulation interval from 90 s to 10 s causes greater depression of field population spike (PS) responses in *Sapap3* KO mice than WT controls. Each stimulation consists of a pair of pulses 50 ms apart. ***A,*** Sample traces of evoked paired stimuli illustrate typical responses at 90 s and 10 s stimulation interval periods in WT and KO mice. Scale bars indicate: 5 ms, 0.5 mV. ***B,*** Time-course plot displays relative change in PS amplitude from 90 s stimulation interval period to 10 s stimulation interval period ($p = 0.005$, rmANOVA). **C,** Summary bar graph compares WT and KO average values over last 10 minutes of 10 s interval stimulation normalized to baseline period ($p = 0.003$, *t*-test). Time-course plot (**D**) and bar graph (**E**) demonstrate a concomitant activity-dependent increase in PPR of PS amplitude in *Sapap3* KO mice ($p = 0.036$, rmANOVA; $p = 0.038$, *t*-test). ***F - J,*** Whole-cell, voltage-clamp recordings of eEPSCs from D2 MSNs show greater activity-dependent synaptic depression in *Sapap3* KO than WT mice. ***F,*** Sample traces illustrate typical responses at 90 s and 10 s stimulation interval periods in WT and KO mice. Scale bars indicate: 20 ms, 200 pA. Time-course plot (**G**) and summary bar graph (**H**) of the normalized eEPSC amplitude ($p = 0.005$, rmANOVA, $p = 0.002$, *t*-test). Time-course plot **(I)** and summary bar graph (**J**) demonstrate a concomitant increase in PPR of eEPSC when stimulation interval is decreased in D2 MSNs of *Sapap3* KO mice ($p = 0.034$, rmANOVA, $p = 0.003$, *t*-test).

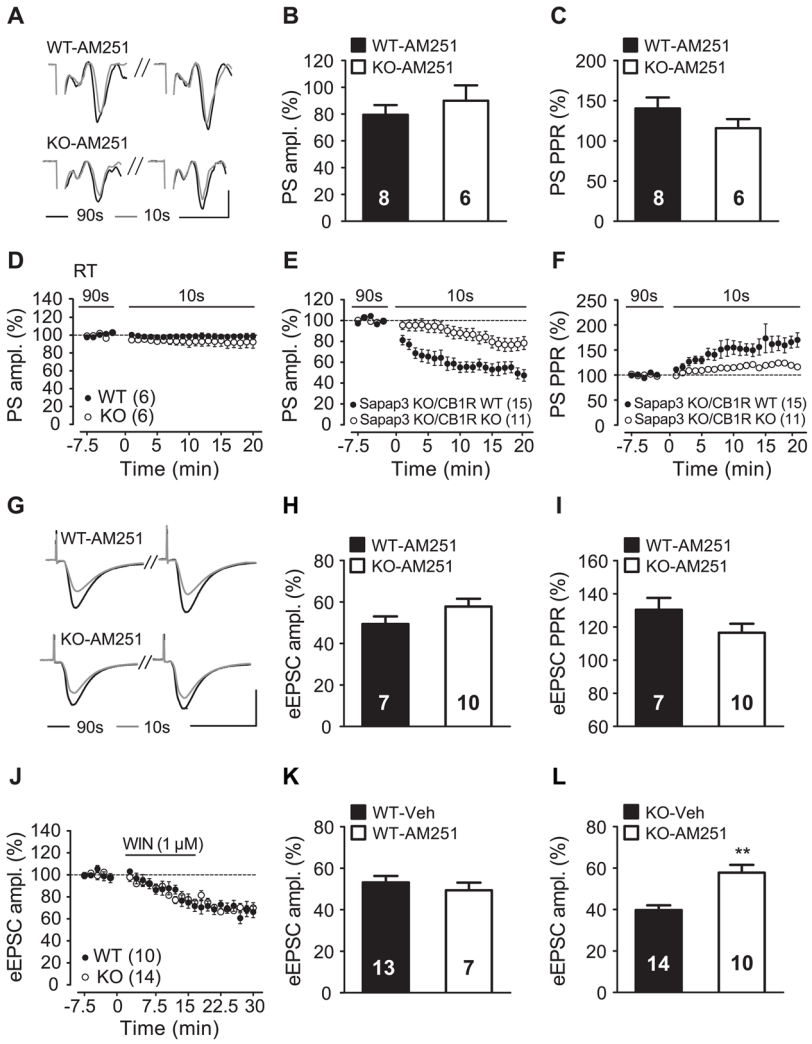

Figure 2. Excessive synaptic depression in *Sapap3* KO mice is mediated by endocannabinoid signaling

A, Sample traces illustrate typical extracellular recording responses in the presence of 3 μM AM251. Scale bars indicate: 5 ms, 0.5 mV. ***B, C,*** AM251 eliminates genotypic differences in activity-dependent depression of PS amplitude (**B**) ($p = 0.434$, *t*-test) and increase in PPR (**C**) ($p = 0.213$, *t*-test). ***D,*** Room temperature prevents activity-dependent depression of PS in *Sapap3* WT and KO mice ($p = 0.316$, rmANOVA). **E,** *CB1R* gene deletion (*CB1R* KO mice) significantly reduces activity-dependent depression of PS amplitude in *Sapap3* KO mice ($p = 0.001$, rmANOVA). **F,** *CB1R* gene deletion significantly reduces activity-dependent increase in PS PPR in *Sapap3* KO mice ($p = 0.023$, rmANOVA). ***G,*** Sample traces illustrate typical eEPSC responses in the presence of 3 μM AM251. Scale bars indicate: 20 ms, 200 pA. ***H,*** In the presence of 3 μM AM251, there is no difference in activity-dependent synaptic depression of D2 MSN eEPSCs between WT and KO ($p = 0.150$, *t*-test). **I,** In the presence of AM251, normalized PPR of KO is no longer greater than WT during the 10 s stimulation interval period ($p = 0.137$, *t*-test). **J,** The CB1R agonist, WIN 55212-2 (1 μM) causes a similar degree of synaptic depression of WT and KO striatal MSN excitatory synaptic responses ($p = 0.791$, rmANOVA). The effects of WIN 55212-2 were tested at room temperature and 90s stimulation interval to avoid unequal contributions by postsynaptically-generated endocannabinoids. **K,** In WT mice, AM251 has no effect on

the degree of activity-dependent depression of D2 MSN eEPSCs ($p = 0.472$, *t*-test). ***L,*** In Sapap3 KO mice, AM251 significantly reduces activity-dependent depression of D2 MSNs eEPSCs ($p = 0.0003$, *t*-test).

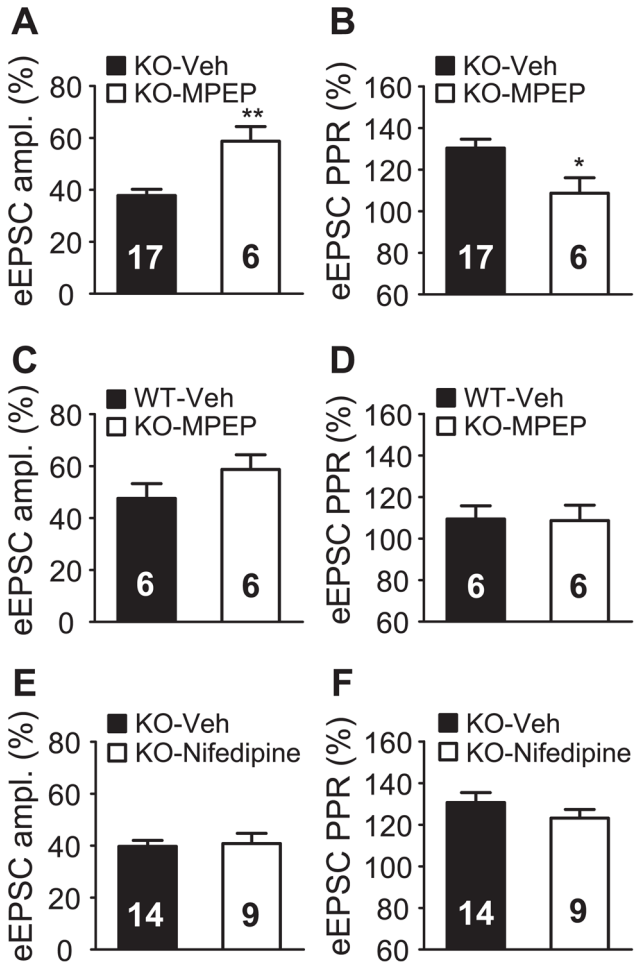

Figure 3. Anomalous eCB-mediated synaptic depression at *Sapap3* KO synapses requires mGluR5

A, Type 5 mGluR antagonist, MPEP (40 μM) significantly reduces activity-dependent depression of D2 MSN eEPSCs in *Sapap3* KO mice ($p = 0.001$, *t*-test). ***B,*** MPEP reduces the activity-dependent PPR increase in D2 MSN eEPSCs of *Sapap3* KO mice ($p = 0.018$, *t*-test). ***C, D,*** Activity-dependent synaptic depression (***C***) and PPR (***D***) in MPEP-treated Sapap3 KO D2 MSNs are similar to untreated WT D2 MSNs, ($p = 0.193$ and 0.942 respectively, *t*-test). ***E, F,*** L-type calcium channel antagonist, nifedipine (10 μM) has no effect on activity-dependent changes in synaptic depression (***E***) or PPR (***F***) of D2 MSN eEPSCs in *Sapap3* KO mice ($p = 0.801$ and 0.291 respectively, *t*-test).

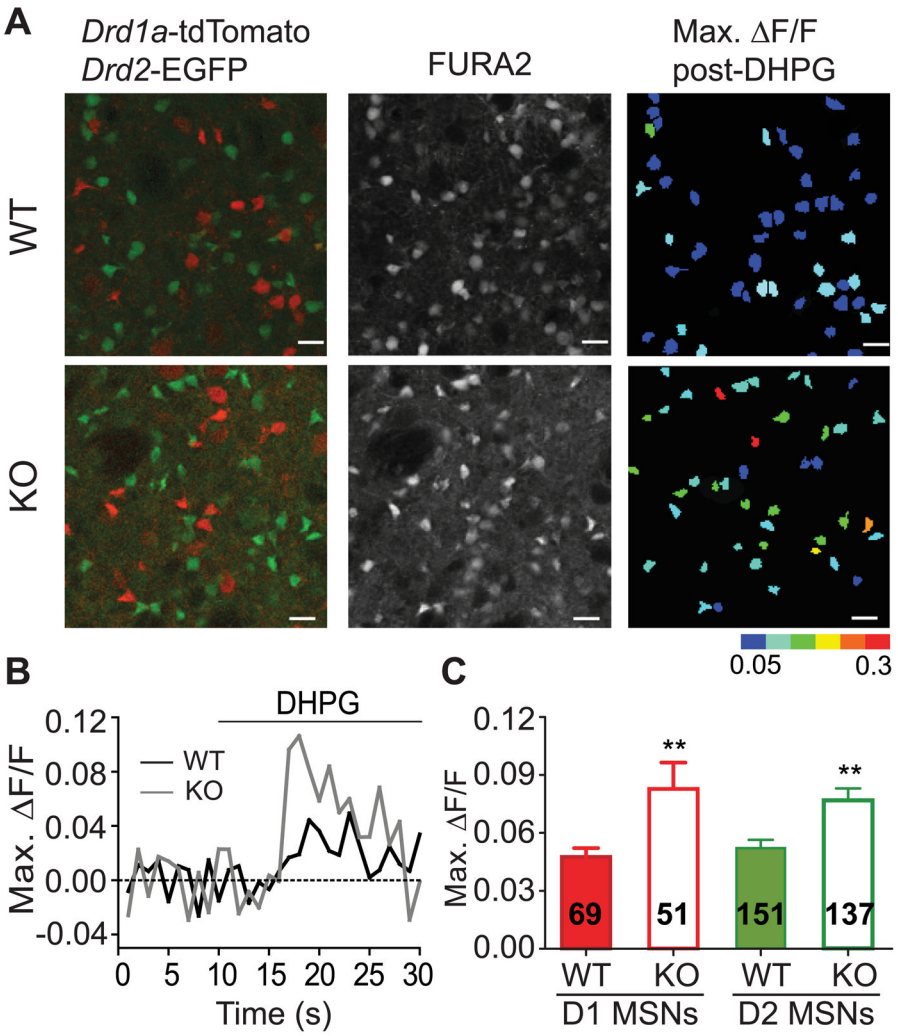

Figure 4. DHPG-induced intracellular calcium transients are increased in striatal MSNs of *Sapap3* KO mice

Intracellular calcium transients are monitored using the cell-permeable, calcium indicator dye, FURA2-AM and two-photon microscopy imaging of acute striatal brain slices. ***A,*** Images show from left to right: overlay of fluorescence from transgenic reporters, *Drd1a*-tdTomato (red) and *Drd2*-EGFP (green); FURA2 fluorescence (basal condition); and pseudo-colored representations of the peak ΔF/F for MSNs in response to DHPG during the 20 seconds after drug application. Pseudo-color scale represents values for ΔF/F in bins of 0.05. Scale bars represent 25 μm. ***B,*** Sample traces of individual MSN fluorescent FURA2 signal in response to DHPG from WT (black) and KO (gray) mice. ***C,*** Post-DHPG peak ΔF/F values are larger in both D1 and D2 MSNs of *Sapap3* KO mice (*n* values refer to cells, $p = 0.002$ for D1 MSNs; $p = 0.001$ for D2 MSNs, *t*-test).

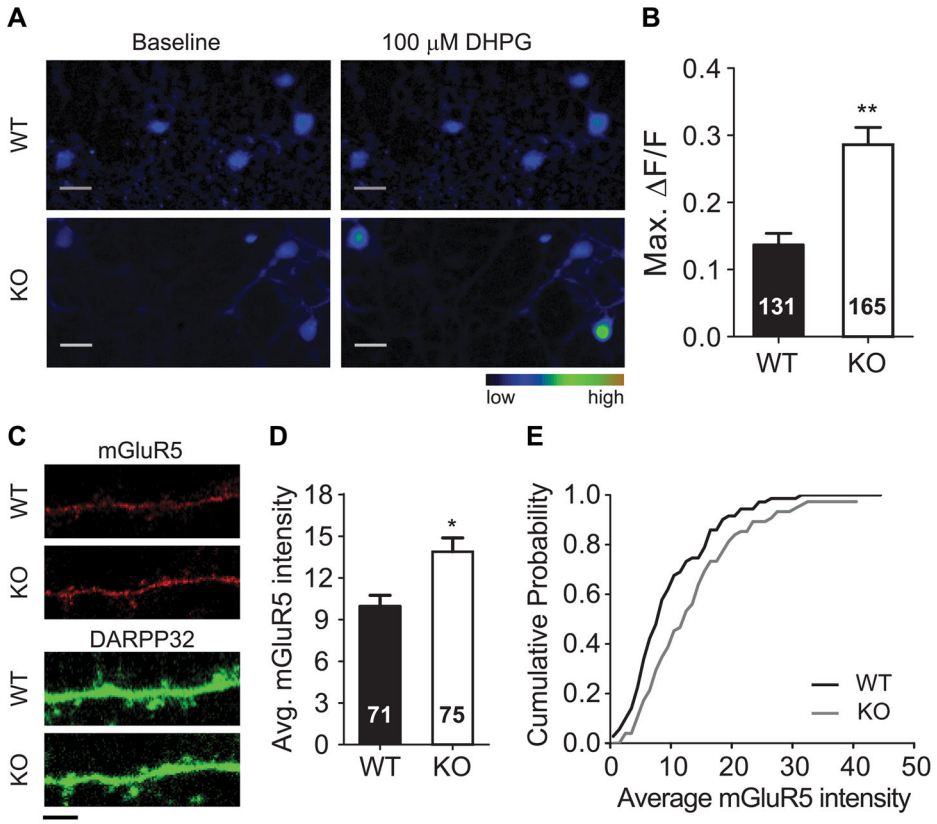

Figure 5. Intracellular calcium transients in response to group 1 mGluR activation and surface expression of mGluR5 are increased in *Sapap3* KO striatal neurons from corticostriatal co-cultures

A, Pseudo-colored images of Fluo-4 intensity in corticostriatal co-cultured neurons from *Sapap3* WT (top) and KO mice (bottom). Sample images correspond to baseline period and 5 s after 100 μM DHPG application. Scale bar indicates 10 μm. ***B,*** Bar graph of the peak Fluo-4 response in the 10 s period following DHPG application demonstrates increased calcium transients in MSNs from *Sapap3* KO cultures (n = 131 cells, 12 wells, 3 culture preparations) relative to WT cultures (n = 165 cells, 13 wells, 3 culture preparations; $p <$ 0.0001, Mann-Whitney test). ***C,*** Example images of mGluR5 surface immunostaining on DARPP32-positive dendritic regions in corticostriatal co-cultures from *Sapap3* WT and KO mice (top panels). DARPP32 staining (pseudo-colored in green) was used to identify medium spiny neurons (bottom panels). Scale bar indicates 5 μm. ***D,*** The average mGluR5 intensity is significantly higher in *Sapap3* KO cultures compared to WT mice (p = 0.003, Mann-Whitney test). ***E,*** Cumulative probability plot shows a rightward shift across all intensities of mGluR5 surface staining of dendritic regions from *Sapap3* KO mice compared to WT mice.

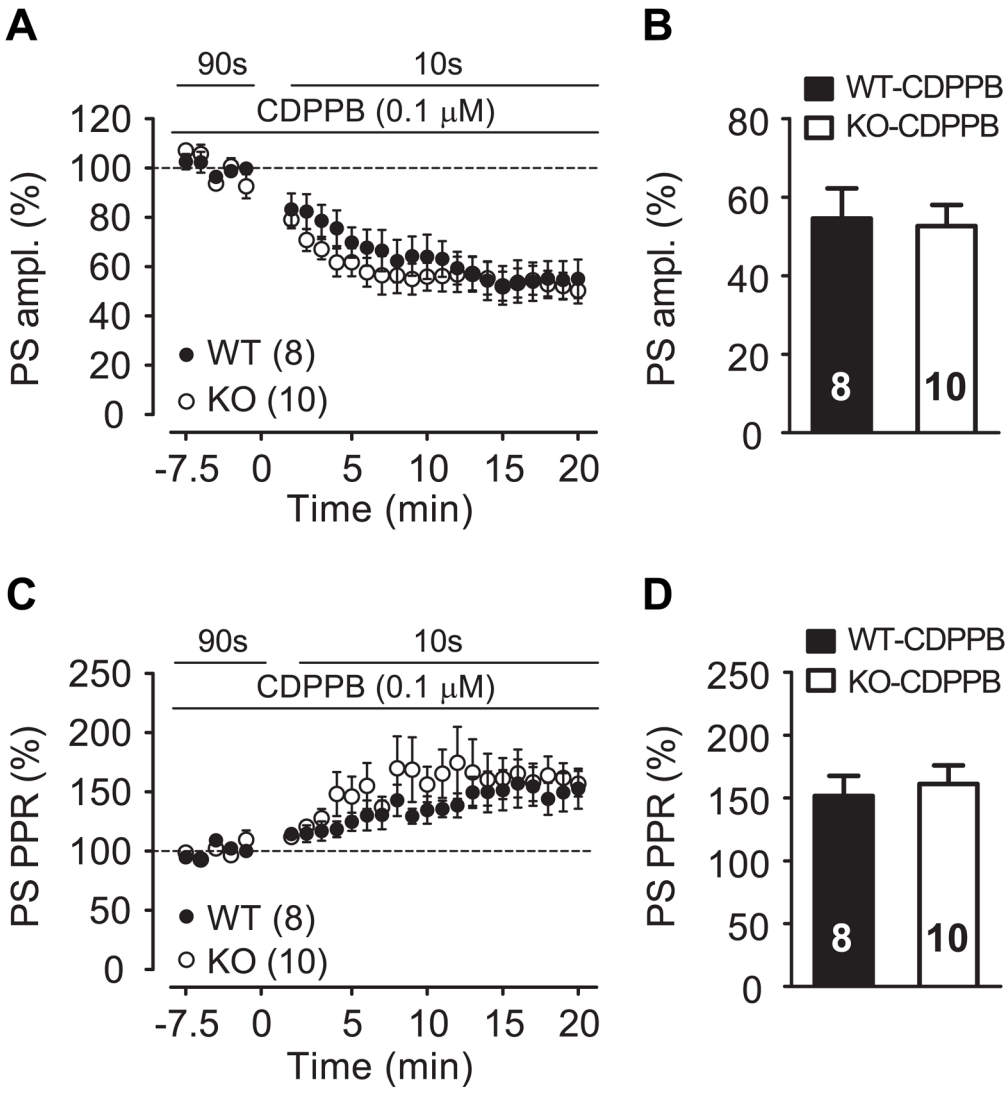

Figure 6. Augmentation of mGluR5 activity by the positive allosteric mGluR5 modulator, CDPPB, during the activity-dependent protocol increases depression of WT responses to KO levels

A, B, In the presence of CDPPB (0.1 μM), the activity-dependent protocol depresses dorsolateral striatal PS field responses of WT and KO mice similarly. Summary bar graphs show the average response during the last 10 minutes of 10s stimulation interval period relative to baseline ($p = 0.541$, rmANOVA*;* $p = 0.836$, *t*-test). **C, D,** In the presence of CDPPB (0.1 μM), the activity-dependent protocol increases PS PPR similarly in WT and KO mice ($p = 0.816$, rmANOVA; $p = 0.664$, *t*-test).

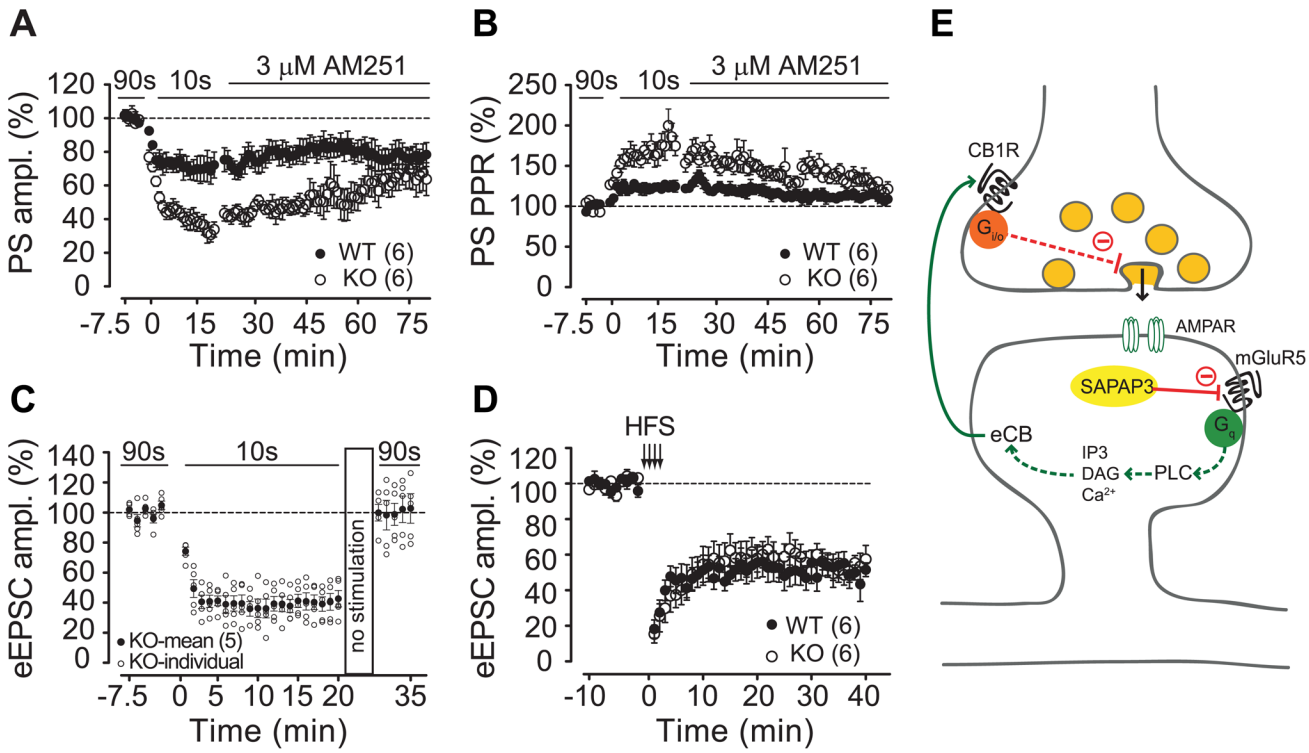

Figure 7. *Sapap3* deletion induces short-term eCB-mediated plasticity, but does not alter magnitude of long-term eCB-mediated plasticity

A, B, In field recordings, AM251 applied after steady-state responses achieved at 10 s stimulation interval reverses the PS depression (***A***) and paired-pulse ratio changes (***B***) of striatal excitatory synapses in *Sapap3* KO to levels indistinguishable from WT mice. Bars indicate periods of stimulation interval and drug application. ***C,*** Pausing stimulation for 10 min. is sufficient to return D2 MSN eEPSCs to basal values when stimulation is resumed at lower rate (90 s interval, 50 ms IPI paired pulses). **D,** There is no difference in the magnitude of LTD elicited between WT and KO D2 MSN eEPSCs ($p = 0.616$, rmANOVA). Arrows indicate time of LTD induction by high frequency stimulation ("HFS", 4 trains of 100 Hz stimulation paired with 0 mV depolarization). ***E,*** Working model depicts SAPAP3 negatively regulating surface levels and activity of mGluR5. In the absence of SAPAP3, increased activity of mGluR5 leads to increased endocannabinoid signaling and inhibition of presynaptic neurotransmitter release.